Journal of Intelligent Systems and Control
https://www.acadlore.com/journals/JISC

Critical Parameter Analysis for Optimized Gliding Performance of Autonomous Underwater Vehicles

Badar Ul Islam[1*], Daim Badar[2], Nasreen Kausar[3]

[1] Electrical Engineering Department, Khawaja Fareed University of Engineering and Information Technology, 64200 Rahim yar Khan, Pakistan
[2] Mechanical and Manufacturing Department, Khawaja Fareed University of Engineering and Information Technology, 64200 Rahim yar Khan, Pakistan
[3] Department of Mathematics, Faculty of Arts and Sciences, Yildiz Technical University, 34220 Esenler, Turkey

[*] Correspondence: Badar Ul Islam (badar.utp@gmail.com)

Received: 06-29-2024 **Revised:** 09-10-2024 **Accepted:** 09-22-2024

Citation: B. Ul Islam, D. Badar, and N. Kausar, "Critical parameter analysis for optimized gliding performance of autonomous underwater vehicles," *J. Intell Syst. Control*, vol. 3, no. 3, pp. 152–159, 2024. https://doi.org/10.56578/jisc030302.

Abstract: Underwater gliders have become a focal point in marine research due to advancements in maritime technologies and the increasing demand for versatile autonomous underwater vehicles (AUVs) in applications such as oceanography, environmental monitoring, and marine surveillance. This study provides a comprehensive analysis of the critical parameters influencing the gliding behavior of a newly designed AUV model, simulated using ANSYS Fluent. In this study, two essential gliding parameters were investigated: the critical angle of attack and the optimum wingspan. The model was fully submerged, and a three-dimensional representation of the AUV was employed to replicate realistic underwater dynamics. Navier-Stokes equations, coupled with continuity equations, were numerically solved to ensure mass and momentum conservation across the simulated environment. The model was rigorously validated against published experimental data, thereby establishing reliability in the simulated outcomes. The results reveal an optimum angle of attack that significantly enhances the glider's maneuverability, facilitating efficient ascent and descent adjustments by the automated control system to navigate precise underwater positions. These findings contribute valuable insights for designing AUVs with enhanced autonomous control and efficient gliding capabilities, aiding in the effective application of AUVs across a range of marine environments.

Keywords: Underwater gliders; Autonomous underwater vehicles; ANSYS fluent simulations; Angle of attack; Optimum control system

1 Introduction

During the last decade, research on underwater vehicles has been the focus around the globe due to their emerging applications, such as their ability to conduct deep-sea inspections, carry out surveys over a long range, conduct oceanographic mapping, monitor and survey underwater pipelines, etc. [1]. The underwater robots are capable of aiding in studying marine and different environment-related challenges and protecting the resources underwater from various pollutants [2]. Underwater gliders fall in the category of 2-meter-long autonomous submersibles and weigh around 50 kg. In terms of shape, they look similar to sailplanes. A typical glider is capable of long-duration tasks (even months spanning to years), and can successfully glide thousands of kilometers in one journey [3]. An underwater glider uses its gravity and buoyant forces to move without requiring any further propulsion. Internal mass is used to realign the glider's position using its center of gravity, resulting in a periodic variation in the glider's pitch angle. The vertical movement due to these modifications in total buoyancy along with the pitch angle is transformed into horizontal motion by using wings attached to each side of the glider. This makes an underwater glider capable of moving forward without the need for any propellers [4]. Compared to the surrounding water, the glider reaches between 0.3 and 0.5 m/s typically as it moves horizontally, while it reaches 0.2 m/s usually in the vertical direction [5]. Currently, the AUVs are now capable of successfully performing missions regarding flying in a particular trajectory through space. These trajectories are mostly simple and in a straight line [6]. The advantages of autonomous data collection are compared against the issues faced by AUVs in terms of sensing, power, information processing, control, and navigation [7]. Perhaps as compared to any other autonomous observing platform, the gliders have the most stringent constraints for the type of sensors they may carry. The key requirements for the glider sensors require them to be small in size and weigh less along with stingy power consumption [8]. Usually, gliders are equipped with conductivity-temperature-depth (CTD) sensors, but an increasing number of other sensors can be installed, such as passive and simple active acoustic sensors, optical (backscatter and fluorescence) sensors, and chemical sensors [9]. Previous research has provided an in-depth analysis of various control methods for AUVs [4]. Those methods are, understandably, based on remote-controlled cruise controllers. It must be known that these systems have taken giant leaps forward and have laid the path for efficient control over AUVs. The Proportional- Integral-Derivative (PID) controller has been used to control the glider's attitude [10]. These feedback-based systems are used in both fully autonomous and semi-autonomous AUVs. They are often used to control the direction of motion and depth of the AUV through buoyancy force. A piston mechanism is connected to the PID controller which sucks and ejects water based on the path requirements, thus altering the buoyancy force and changing the course of the AUV. The Linear Quadratic Regulator (LQR) controller has also been used to control the glider's motion [11]. Even though the control systems previously proposed in research demonstrate satisfactory control performance, they still face issues in compensating for the high nonlinearity of underwater vehicles and disturbances. These primary reasons make it difficult to control the underwater gliders [12].

As AVU systems mature to a point at which they may be commercialized, the importance of cost reliability and robustness is gaining extended significance. More and more global corporations are showing interest in novel technology. The incorporation of AUVs in various industries and research fields has become inevitable. The pace, at which several new factions of ocean research, preservation, and maritime operations have evolved over the last couple of decades, has encouraged the consolidation of improvised scientific techniques such as the use of AUVs. It can be safely said that the coming years will bring about massive reforms in the existing AUV control systems and design. An intensive literature review shows that the majority of the existing literature revolves around the computational features of AUVs. Moreover, it has also been observed that control systems have occupied the center stage when it comes to AUV research. This study focuses on discussing, studying, and analyzing various design parameters of AUVs and their subsequent effects on the glider performance. The critical angle of attack for various wingspans was critically studied [13]. This study provides crucial information on the impact of a change in wingspan on glider performance.

2 Methodology

For the numerical simulations, a solid three-dimensional model of the underwater glider was made on the CAD software, SolidWorks. Solutions presented the calculation of using a high decision advection scheme. The residual mass errors were decreased to four orders of value and lift and drag forces on the AUV were evaluated to achieve convergence. Common run times were wall clock hours for absolutely submerged instances and twelve hours for simulations consisting of the unfastened surface [14].

2.1 Simulation Setup

The fluid domain was designed to simulate the environment around the underwater glider. As recommended by the study [13], the inlet was kept at 10D (D denotes the diameter of the glider) moreover the vent was suggested to be kept above 15D to evade the impact of the borders. In the current study, the fluid domain was 5L glider $\times$ 16D glider $\times$ 16D glider was used. There was 2L glide from the intake and 3L glider from the outlet, whereas, the bottom and bottom of the domain were kept at 8D from the glider respectively. The mesh size was 300 mm and the k-ϵ turbulence model was selected under the following conditions.

The velocity of the fluid at the inlet velocity was maintained at 0.3 m/s with the water having 998 kg/m^3. The pressure at the outlet was set to zero Pa. Additionally, the boundary condition of the no-slip wall was used. The fluid's density and velocity remained unchanged during the simulations.

2.2 Dynamic Modeling

When an underwater glider steers through the ocean water, it is subjected to both external and internal forces and moments due to the moving mass on the inside. These forces play a critical role in the assessment of the overall dynamics of the glider. Zhang et al. [10] examined the steady-state motion of an underwater glider by conducting practical experiments. The examined glider was subject to the mentioned forces. Furthermore, several researchers worked on an underwater glider employing dynamic modeling [15, 16]. Figure 1 shows the distribution of mass, providing a comprehensive understanding of the forces acting upon the glider.

The total mass of the glide can be expressed as the sum of all the individual masses present in the glider. The total mass of the glider can be expressed as follows:

$$m_v = m_h + m_w + m_b + \overline{m} \tag{1}$$

where, m_v is the total mass of the glider; m_h is the uniformly distributed hull mass; m_w is the point mass with displacement r_w; m_b is the variable ballast mass; and $\bar{m}$ is the moveable mass with vector r_p.

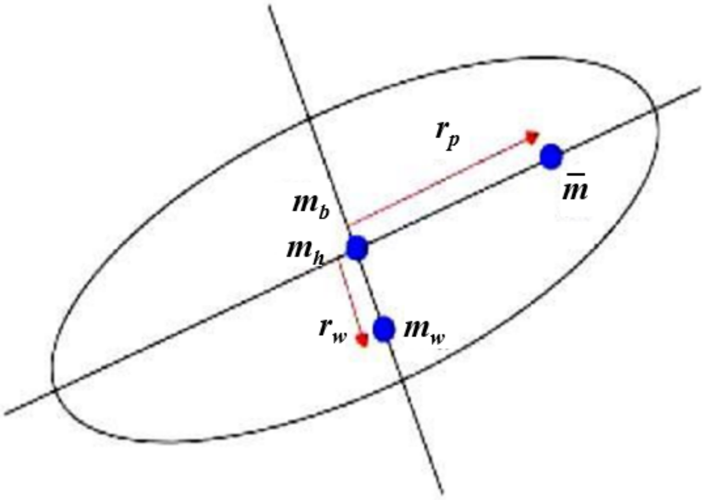

Figure 1. Distribution of mass

The fluid that is displaced has a mass.

$$m_o = m_v - m \tag{2}$$

where, m_o is the mass of the displaced fluid.

In terms of the mathematical modeling of the glider, Seo et al. [17] which derived the generalized expression for the dynamic model for an underwater glider as well as for the internal mass of motion.

Newton's laws served as the basis for the simplification of these formulations. Using the following equations, these equations can be simplified along the longitudinal plane Eqs. (3)-(5) [18]:

$$v_x = \frac{1}{m_1}\left[-m_3 v_z \Omega_2 - m_o g \sin\theta + L\sin\alpha - D\cos\alpha - u_x\right] \tag{3}$$

$$v_z = \frac{1}{m_3}\left[m_1 v_x \Omega_2 + m_o g \cos\theta - L\cos\alpha - D\sin\alpha - u_z\right] \tag{4}$$

$$\begin{aligned}\Omega = \frac{1}{I_2}&\left[(m_3 - m_1)\, v_x v_z - \bar{m} g\left(r_{px}\cos\theta + r_{pz}\sin\theta i + M_{DL2} - rp_z u_x + rp_x u_z - \right.\right.\\ &\left.\left.\Omega_2\left(r_{px}p_{px} + r_{pz}p_{pz}\right)\right)\right]\end{aligned} \tag{5}$$

where, v_x and v_z are the longitudinal components of velocity V; θ is the pitch angle; and Ω is the angular velocity. The angle of attack is calculated as follows:

$$a = \tan^{-1}\frac{v_z}{v_x} \tag{6}$$

The translational velocity stays constant and the angular velocity is zero when there is steady motion.

$$\alpha = \frac{K_{LO}}{K_L} \pm \sqrt{\left(\frac{K_{LO}}{K_K}\right)^2 + \frac{K_{DO}}{K_D}} \tag{7}$$

$$\tan\theta = -\frac{D}{L} = -\frac{K_{DO} + K_D\alpha^2}{K_{LO} + K_L\alpha} \tag{8}$$

$$v = \frac{\sqrt{m_o g}}{\left[L(\alpha)^2 + D(\alpha)^2\right]^{1/4}} \tag{9}$$

where, D and L represent the drag and lift, respectively, and depend on α.

2.3 Hydrodynamic Forces

The gliding behavior of the glider is heavily influenced by the nature of hydrodynamic forces acting upon it. These forces majorly include the drag (D) and lift (L) forces [19, 20]. These forces are reliant on the angle of attack as follows:

$$D = \left[K_{DO} + K_D(\alpha)^2\right] v^2 \tag{10}$$

$$L = (K_{LO} + K_L \alpha)\, v^2 \tag{11}$$

$$M = (K_{MO} + K_M \alpha)\, v^2 \tag{12}$$

where, K_{DO} and K_D represent the drag coefficients; K_{LO} and K_L are the lift coefficients; and K_{MO} and K_M are the moment coefficients.

3 Results

After an arduous effort of acquiring the required skill set to perform meaningful analysis, it was initiated to implement the attained knowledge on the simulation software. An extensive streak of simulations was run on the software. The whole process was divided into three distinctive parts. The overall simulation results were a conglomerate of those individual parts. To streamline the simulation process, the analysis was run on a simple two-dimensional body in the beginning which laid a foundation for the simulation to build upon. The second step involved the simulation procedure for analyzing the glider's wing. The individual analysis of the wing helped in determining the overall gliding behavior. The third and final step of the analysis was run on the glider's complete body. Figure 2 shows the result of an analysis run on a two-dimensional airfoil. It is the pressure distribution on the airfoil surface.

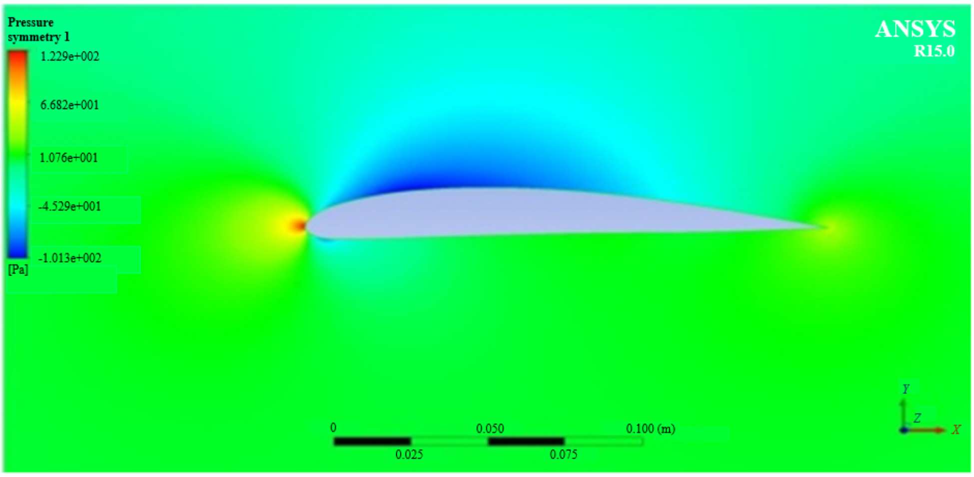

Figure 2. Pressure distribution on airfoil

As Figure 2 suggests, compared to the bottom surface, the pressure on the upper surface was much lower which accounted for the lift force generated due to the pressure difference. This might happen due to the asymmetric shape around the longitudinal axis of the airfoil. The upper surface provided air with a smooth flowing surface, whereas the lower surface broke the streamlines of air. The inverse relation between pressure and velocity came into effect and approved the trends of pressure distribution. Figure 3 presents the velocity distribution on the airfoil surfaces.

It can be seen that the velocity on the upper face was higher compared to the bottom face. This figure can be understood as the reciprocal of Figure 2. The points where the pressure values were maximum had the lowest velocity values, and vice versa. In Figure 4, the red line represents the top surface of the airfoil and displays lower pressure values, whereas the blue line represents the bottom surface of the airfoil and shows the higher value of pressure.

The second part of the analysis focused on running the simulations on the wing of the glider to find the coefficient values of lift and drag for the wing. Figure 5 presents the pressure contour distribution over the wing plane of the glider.

Analysis was run for different angles of attack for the wing with a step of 3°. Contours are shown below for a simple understanding of the results. Several variations on the wing were made to calculate the critical parameters that determine the ultimate maneuverability of the glider. Different angles of attack were set for the wing and simulations were run. A change in the angle of attack changed the pressure distribution contours on the wing (Figure 5). As the angle of attack increased, the pressure on the top surface decreased. As the angle of attack increased, the pressure on the top surface decreased proportionally. After the proper study of the airfoil and wing, a set of analyses was run for the glider body. During the glider analysis, an intricate study of the critical parameters was carried out. Figure 6 shows the effect of a positive 9° angle of attack on the pressure contours of the glider. This figure shows that the point of concentration moved further down the nose as the attacking fluid made first contact with the glider at that point. This angle of attack was beyond the critical angle of attack of the glider. At this angle of attack, the value of the drag coefficient started to decrease suddenly.

Figure 7 and Figure 8 were plotted for the simulation results to calibrate and evaluate the results of the analysis.

As shown in Figure 7, the value of the lift coefficient increased with the increase in the angle of attack, but started decreasing at a certain angle (12°) of attack. That point is called the critical angle of attack. If the angle of attack of the glider is increased beyond the critical angle of attack, the glider can stall, which means that its nose can start to point start-up (or down), depending on the nature of the angle of attack and the glider can lose its path. Such a situation can cause severe body damage. If a recalibration and balancing system is not installed in the glider, the glider may sink to the ocean floor. Thus, when the glider is to be taken to a specific location in the ocean, the nose of the glider cannot be tilted more than ±15°. This parameter helps a great deal in scheduling the gliding path for the glider. Figure 8 shows the lift coefficient (C_l) against the drag coefficient (C_d). They clearly show a trend of direct proportionality and, thus, this concludes that these values increase with the increase in the angle of attack. The same trends were shown by these values on both sides of the datum line, i.e., the origin line. The values hold onto their trend whether the value of the angle of attack is positive or negative.

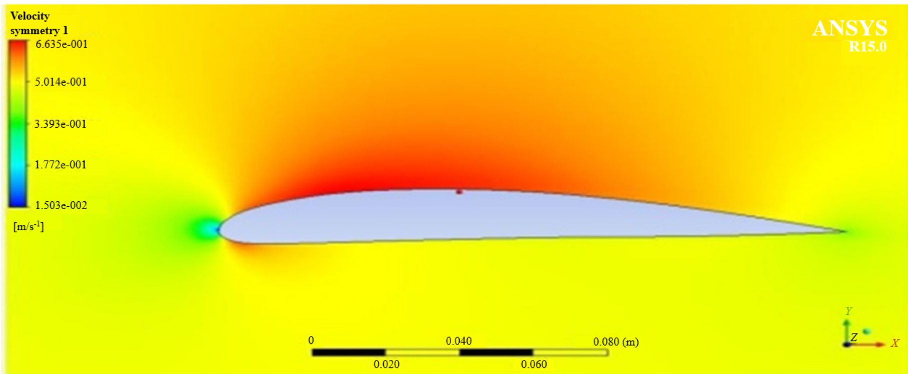

Figure 3. Velocity distribution

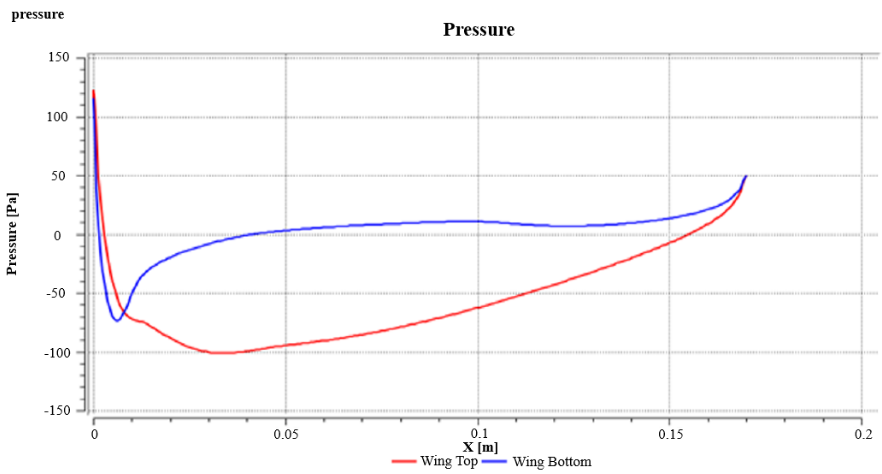

Figure 4. Pressure distribution graph

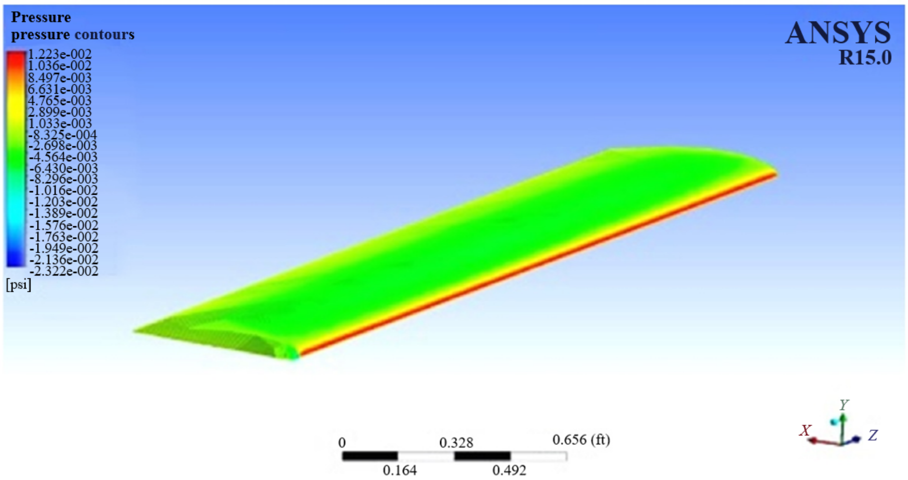

Figure 5. Pressure contour distribution over the wing plane of the glider

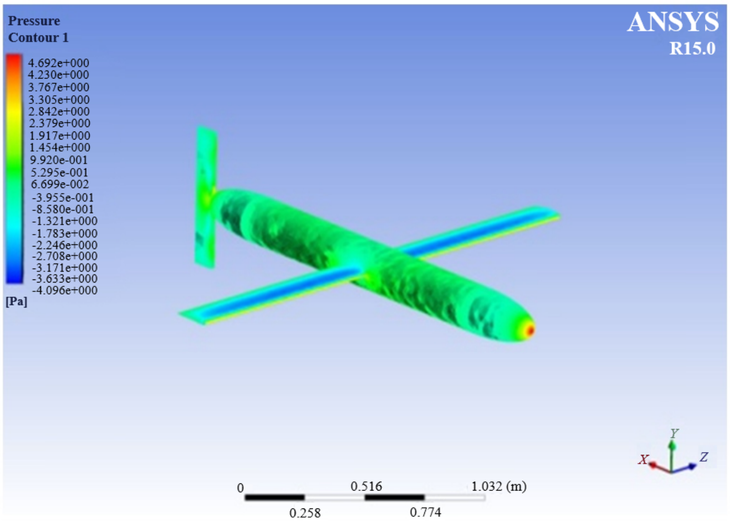

Figure 6. Pressure contour distribution over the glider body

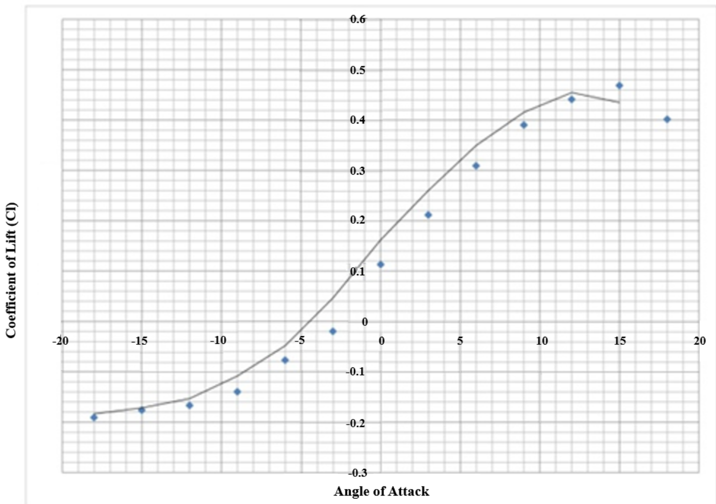

Figure 7. Illustration of the lift coefficient against the angle of attack

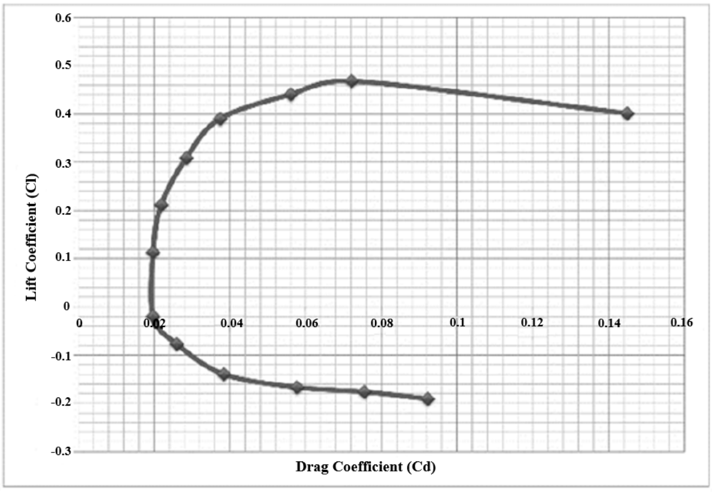

Figure 8. Illustration of the lift coefficient against the drag coefficient

4 Conclusions

This study provides the values for parameters that are critical for the maneuverability of the glider. These parameters include the values of Cd and Cl and the critical angle of attack. The critical angle of attack was found to be 15°. This angle helps the automated control system to dip or lift the nose of the glider when it has to move to a certain point in the ocean. This study can be used as the takeoff point to increase the angle of attack for this glider and thus make it easier and more flexible in terms of maneuverability.

This study establishes a solid basis for future investigation and advancement in this field. The glider's flexibility and responsiveness during flight could be greatly improved by pushing the critical angle of attack's boundaries past the present threshold. By increasing this angle of attack, the glider may be able to achieve greater control dynamics, more accurate maneuvering, more energy efficiency, and a wider variety of operational capabilities.

Data Availability

Not applicable.

Conflicts of Interest

The authors declare no conflict of interest.

References

[1] R. Kot, "Review of collision avoidance and path planning algorithms used in autonomous underwater vehicles," *Electronics*, vol. 11, no. 15, p. 2301, 2022. https://doi.org/10.3390/electronics11152301

[2] S. Siregar, B. R. Trilaksono, E. M. I. H. Hidayat, M. Kartidjo, N. Habibullah, M. F. Zulkarnain, and H. N. Setiawan, "Design and construction of hybrid autonomous underwater glider for underwater research," *Robotics*, vol. 12, no. 1, p. 8, 2023. https://doi.org/10.3390/robotics12010008

[3] M. F. bin Ibrahim, O. Mark, and K. bin Shehabuddeen, "An underwater glider for subsea intervention: A technical feasibility study," *Appl. Mech. Mater.*, vol. 393, pp. 561–566, 2013. https://doi.org/10.4028/www.scientific.net/AMM.393.561

[4] I. Bae and J. Hong, "Survey on the developments of unmanned marine vehicles: Intelligence and cooperation," *Sensors*, vol. 23, no. 10, p. 4643, 2023. https://doi.org/10.3390/s23104643

[5] J. G. Graver, "Underwater gliders: Dynamics, control and design," doctoralthesis, Princeton University, 2005.

[6] C. X. Lyu, D. Lu, C. K. Xiong, R. Hu, Y. F. Jin, J. H. Wang, Z. Zeng, and L. Lian, "Toward a gliding hybrid aerial underwater vehicle: Design, fabrication, and experiments," *J. Field Robot.*, vol. 39, no. 5, pp. 543–556, 2022. https://doi.org/10.1002/rob.22063

[7] K. Isa, M. R. Arshad, and S. Ishak, "A hybrid-driven underwater glider model, hydrodynamics estimation, and an analysis of the motion control," *Ocean Eng.*, vol. 81, pp. 111–129, 2014. https://doi.org/10.1016/j.oceaneng.2014.02.002

[8] X. Tian, H. W. Zhang, L. H. Zhang, Y. H. Wang, Y. H. Liu, and Y. Yang, "Research on positive buoyancy underwater glider and its sailing efficiency," *Appl. Ocean Res.*, vol. 110, p. 102592, 2021. https://doi.org/10.1016/j.apor.2021.102592

[9] D. H. Ji, H. S. Choi, J. I. Kang, H. J. Cho, M. G. Joo, and J. H. Lee, "Design and control of hybrid underwater glider," *Adv. Mech. Eng.*, vol. 11, no. 5, 2019. https://doi.org/10.1177/1687814019848556

[10] B. B. Zhang, D. X. Ji, S. Liu, X. K. Zhu, and W. Xu, "Autonomous Underwater Vehicle navigation: A review," *Ocean Eng.*, vol. 273, p. 113861, 2023. https://doi.org/10.1016/j.oceaneng.2023.113861

[11] N. E. Leonard and J. G. Graver, "Model-based feedback control of autonomous underwater gliders," *IEEE J. Ocean. Eng.*, vol. 26, no. 4, pp. 633–645, 2001. https://doi.org/10.1109/48.972106

[12] N. E. Leonard, D. A. Paley, R. E. Davis, D. M. Fratantoni, F. Lekien, and F. M. Zhang, "Coordinated control of an underwater glider fleet in an adaptive ocean sampling field experiment in monterey bay," *J. Field Robot.*, vol. 27, no. 6, pp. 718–740, 2010. https://doi.org/10.1002/rob.20366

[13] J. H. Li and P. M. Lee, "Design of an adaptive nonlinear controller for depth control of an autonomous underwater vehicle," *Ocean Eng.*, vol. 32, no. 17-18, pp. 2165–2181, 2005. https://doi.org/10.1016/j.oceaneng.2005.02.012

[14] L. Merckelbach, D. Smeed, and G. Griffiths, "Vertical water velocities from underwater gliders," *J. Atmos. Ocean. Tech.*, vol. 27, no. 3, pp. 547–563, 2010. https://doi.org/10.1175/2009JTECHO710.1

[15] J. Muhammad Yasar, O. Mark, T. Nagarajan, S. S. A. Ali, and U. Barkat, "Study on wing aspect ratio on the performance of a gliding robotic fish," *Appl. Mech. Mater.*, vol. 786, pp. 248–253, 2015. https://doi.org/10.4028/www.scientific.net/AMM.786.248

[16] D. L. Rudnick, R. E. Davis, C. C. Eriksen, D. M. Fratantoni, and M. J. Perry, "Underwater gliders for ocean research," *Mar. Technol. Soc. J.*, vol. 38, no. 2, pp. 73–84, 2004. https://doi.org/10.4031/002533204787522703

[17] D. C. Seo, G. Jo, and H. S. Choi, "Pitching control simulations of an underwater glider using CFD analysis," in *OCEANS 2008 - MTS/IEEE Kobe Techno-Ocean*, Kobe, Japan, 2008, pp. 1–5. https://doi.org/10.1109/OCEANSKOBE.2008.4530978

[18] P. Yu, T. Wang, H. Zhou, and C. Shen, "Dynamic modeling and three-dimensional motion simulation of a disk type underwater glider," *Int. J. Nav. Archit. Ocean Eng.*, vol. 10, no. 3, pp. 318–328, 2018. https://doi.org/10.1016/j.ijnaoe.2017.08.002

[19] J. Neira, C. Sequeiros, R. Huamani, E. Machaca, P. Fonseca, and W. Nina, "Review on unmanned underwater robotics, structure designs, materials, sensors, actuators, and navigation control," *J. Robot.*, vol. 2021, no. 1, p. 5542920, 2021. https://doi.org/10.1155/2021/5542920

[20] F. T. Zhang, J. Thon, C. Thon, and X. B. Tan, "Miniature underwater glider: Design, modeling, and experimental results," in *2012 IEEE International Conference on Robotics and Automation*, Saint Paul, MN, USA, 2012, pp. 4904–4910. https://doi.org/10.1109/ICRA.2012.6225264